Journal of Environmental Management 405 (2026) 129710

Contents lists available at ScienceDirect

Journal of Environmental Management

journal homepage: www.elsevier.com/locate/jenvman

Research article

Dark sky protection in high-density urban fringe areas: Site suitability assessment for dark sky parks and light environment optimization strategies—a case study of Guangzhou

Benyan Jiang [a,d], Kailing Xu [a], Zihao Zheng [b,*], Jianjun Li [a,**], Hongguang Wang [c,d], Lin Mei [e]

[a] School of Architecture and Urban Planning, Guangzhou University, Guangzhou 510006, China
[b] School of Geography and Remote Sensing, Guangzhou University, Guangzhou 510006, China
[c] School of Physics and Materials, Guangzhou University, Guangzhou 510006, China
[d] Sub-center of the Greater Bay Area, National Astronomical Science Data Center, Guangzhou 510006, China
[e] Shenzhen Astronomical Observatory, Shenzhen 518040, China

ARTICLE INFO

Keywords:
High-density urban area
Dark sky park
Site selection
Light pollution
Guangzhou

ABSTRACT

With the acceleration of global urbanization, high-quality dark sky resources are becoming increasingly scarce. As the intersection of the front line of light pollution diffusion and ecological buffer zones, the urban fringe of megacities faces dark sky protection challenges arising from complex baseline light environments and intensified human activities. Taking Guangzhou as a case study, this paper proposes a dark sky park site selection and light environment optimization framework based on multi-source data integration. By integrating high-resolution nighttime light remote sensing data from SDGSAT-1, ground-based SQM measurements, all-sky fish-eye imagery, and POI-based socio-perceptual data, a multi-dimensional site suitability evaluation model is constructed, incorporating natural baseline conditions, transportation accessibility, and socio-economic factors. The results indicate that (1) distinct "dark sky islands" are present in northeastern Guangzhou, and a total of 13 natural protected areas with potential for dark sky park development were identified, among which Conghua Lianxi Municipal Forest Park exhibits the highest overall suitability with a score of 0.89; (2) Ground-based measurements confirm that under moonless conditions the zenith night sky brightness in this area reaches up to 21.28 mag/arcsec^2, meeting the Dark-Sky International (IDA) Silver Tier standard ($21.00 \leq SQM \leq 21.74$), with the optimal observation window occurring between 02:00 and 05:00; (3) POI-based source attribution analysis reveals that near-horizontal light pollution is primarily generated by the adjacent Shantou-Zhanjiang Expressway as a linear source, while public service facilities within the protected areas exhibit characteristics of high-intensity point light sources. Based on these findings, this study proposes an integrated optimization pathway that combines top-down and bottom-up approaches, providing quantitative evidence and a practical framework for constructing dark sky ecological networks in the urban fringe of megacities.

1. Introduction

With the continued acceleration of global urbanization, artificial light at night (ALAN) has expanded rapidly. As an emerging anthropogenic environmental exposure factor, nighttime light has transformed light pollution into an increasingly severe environmental issue on a global scale (Kyba et al., 2017). A substantial body of research demonstrates that the persistent intensification of ALAN disrupts the circadian rhythms of natural ecosystems and threatens the survival nocturnal species (Gaston and Sánchez, 2022; Hirt et al., 2023; Ścięžor et al., 2025), while exerting potential adverse impacts on human health and social well-being (Linares Arroyo et al., 2024; Navara and Nelson, 2007). Another obvious impact is the extensive disappearance of natural starry skies. More than one-third of the global population is currently unable to observe the Milky Way with the naked eye, while night sky brightness in the core areas of certain high-density cities has surged to

* Corresponding author.
** Corresponding author.
E-mail addresses: zhengzh@gzhu.edu.cn (Z. Zheng), Lijianjun@gzhu.edu.cn (J. Li).

https://doi.org/10.1016/j.jenvman.2026.129710
Received 8 January 2026; Received in revised form 14 April 2026; Accepted 15 April 2026
Available online 19 April 2026

levels tens of times higher than the natural background (Falchi et al., 2016). Against this backdrop, striking a balance between urban development imperatives and dark sky conservation, has emerged as a pivotal scientific and governance issue requiring an urgent response within the realm of global sustainable development.

To mitigate the ecological risks associated with ALAN and enhance awareness regarding the hazards of light pollution, institutions such as the Dark-Sky International (IDA) have spearheaded the establishment of a system of dark sky places, typified by "Dark Sky Parks" (International Dark-Sky Association, 2018); these initiatives aim to preserve night sky quality through spatial delineation and lighting controls (Baack et al., 2024), while simultaneously exploring methodologies to translate dark sky resources into an integration of ecological conservation and nature education (Supriya & Kumar, 2023). Although twenty-two countries worldwide have established dark sky protected areas, and China has begun to explore pathways for converting starry sky resources into ecological products (Zhong et al., 2019), existing research and practices exhibit significant geographical limitations. Current scholarship on dark sky conservation is predominantly focused on sparsely populated western regions or ecologically fragile remote areas, such as the Qinghai-Tibet Plateau and western deserts (Wei et al., 2019; Zhu et al., 2021). In contrast, there is a notable scarcity of research concerning dark sky conservation in the urban fringes of metropolises, despite these areas facing more severe light pollution threats and possessing a greater urgency for intervention (Li et al., 2025).

Compared with regions of low human disturbance, the sources of light pollution within the urban fringe are significantly more complex (Horynek, 2024; So et al., 2025); they encompass both high-intensity point sources, such as rural settlements, and widespread area sources resulting from the aggregation of infrastructure and human activities in towns (Chang et al., 2025; Feng et al., 2022). The nocturnal light environment in these areas is often characterized by the coexistence of elevated background brightness, strong spatial heterogeneity, and significant temporal dynamic variations (Liu et al., 2025). Against this backdrop, traditional site selection methodologies for dark sky parks, which rely on singular nighttime light remote sensing data or empirical thresholds, are ill-suited for the complex light environment scenarios found in highly urbanized contexts (Li et al., 2026; Liu et al., 2023). Simultaneously, when wide-area urban lighting constitutes the primary source of light for dark sky parks, the bottom-up lighting optimization approach developed by the IDA—centered on the control of lighting fixtures—proves relatively inefficient; this necessitates the pursuit of an integrated optimization strategy that combines top-down measures, such as urban planning, with bottom-up interventions, such as lighting facilities management (Barentine, 2022).

From a technical perspective, site selection for dark sky parks and the optimization of the nocturnal light environment in the urban fringe face two primary challenges: (1) how to accurately identify dark sky patches with potential conservation value under conditions of intense light pollution noise (Zheng et al., 2025); and (2) how to elucidate the coupling relationships between diverse human activity factors—such as transportation networks, village distributions, and public infrastructure—and the spatial patterns of light pollution (Jiang et al., 2022). Existing scholarship predominantly relies on single-scale nighttime light remote sensing or ground-based observational data, lacking the integrated utilization of "sky-ground" multi-source observational data; this deficiency restricts the refined tracing and quantitative analysis of light pollution sources (Zheng et al., 2025). Consequently, constructing a suitability evaluation framework for dark sky park site selection tailored to highly urbanized regions, and conducting a comprehensive analysis by integrating multi-source remote sensing data, ground-based measurements, and human activity data, holds urgent scientific significance and meets pressing practical demands (Wei et al., 2019).

As a core city in the Guangdong-Hong Kong-Macao Greater Bay Area, Guangzhou exhibits a nocturnal light environment characterized by typical spatial differentiation: light pollution is highly concentrated in the central urban area (Yang et al., 2021), whereas the northern regions retain a relatively intact natural ecological background, forming a distinct "urban-nature" transition pattern. This typical metropolitan fringe structure provides an ideal research scenario for exploring dark sky conservation and spatial optimization pathways within a megacity. Accordingly, this study takes Guangzhou as a case study with the aim of achieving the following objectives: (1) to comprehensively integrate high-precision nighttime light remote sensing with multi-dimensional ground-based measurement techniques to construct a suitability evaluation model for dark sky park site selection applicable to highly urbanized areas; (2) to quantitatively analyze the sources of light pollution and their spatial distribution characteristics in the target area by combining Point of Interest (POI) data with fish-eye; (3) to propose optimization pathways for the nocturnal light environment that integrate top-down policy regulation with bottom-up community co-governance, based on the results of the spatial analysis.

By situating dark sky conservation within the framework of spatial governance and environmental risk control in a highly urbanized context, this study not only extends the regional dimensions of existing research but also provides a theoretical foundation and practical paradigm that serve as a reference for metropolitan fringes worldwide in seeking a balance between ecological conservation and the synergistic development of the dark sky economy.

2. Study area and data

2.1. Study area

Serving as the core engine of the Guangdong-Hong Kong-Macao Greater Bay Area (GBA), Guangzhou (112°57′E–114°03′E, 22°26′N–23°56′N) stands as a quintessential ultra-high-density megacity. Guangzhou administers 11 administrative districts with significant spatial differences in development and ecological patterns. The central urban area, characterized by flat terrain and high building density, serves as the core functional agglomeration zone. Conversely, the northern region (represented by Conghua District) features high forest coverage and mountainous terrain with low development intensity, functioning as an important ecological barrier for the city. Akin to most international metropolises, the luminous environment of Guangzhou exhibits a pronounced "Core-Periphery Spatial Differentiation" (Wu et al., 2025). The central urban area is characterized by high intensity and extreme levels of ALAN. In contrast, the northern districts of Conghua and Zengcheng leverage their mountainous terrain as a natural barrier, which effectively attenuates the intrusion of light pollution from the city center and preserves a relatively intact natural dark sky baseline. (Fig. 1-A/B/C/D). This pronounced gradient variation in the light environment renders Guangzhou an ideal case study for exploring dark sky conservation model within the context of high urbanization.

This study focuses on the system of nature protected areas within the administrative boundaries of Guangzhou. Characterized by a subtropical monsoon climate, the region experiences high rainfall and significant cloud cover in summer, whereas winters are relatively dry and clear; these climatic conditions not only influence biological rhythms but also dictate the seasonal window for dark sky observation (aligning with the observation period from December to June mentioned subsequently). Based on vector data provided by the Forestry Administration of Guangdong Province, the scope of this study encompasses 89 nature protected areas in Guangzhou, comprising nature reserves, forest parks, and wetland parks. These protected areas are primarily distributed along the northern mountain ranges and eastern water systems; notably, Conghua District and Zengcheng District possess the highest concentration of protected areas and exhibit a high degree of spatial overlap with regions of low light pollution (Fig. 1-E), serving as core vectors for constructing the urban dark sky ecological network.

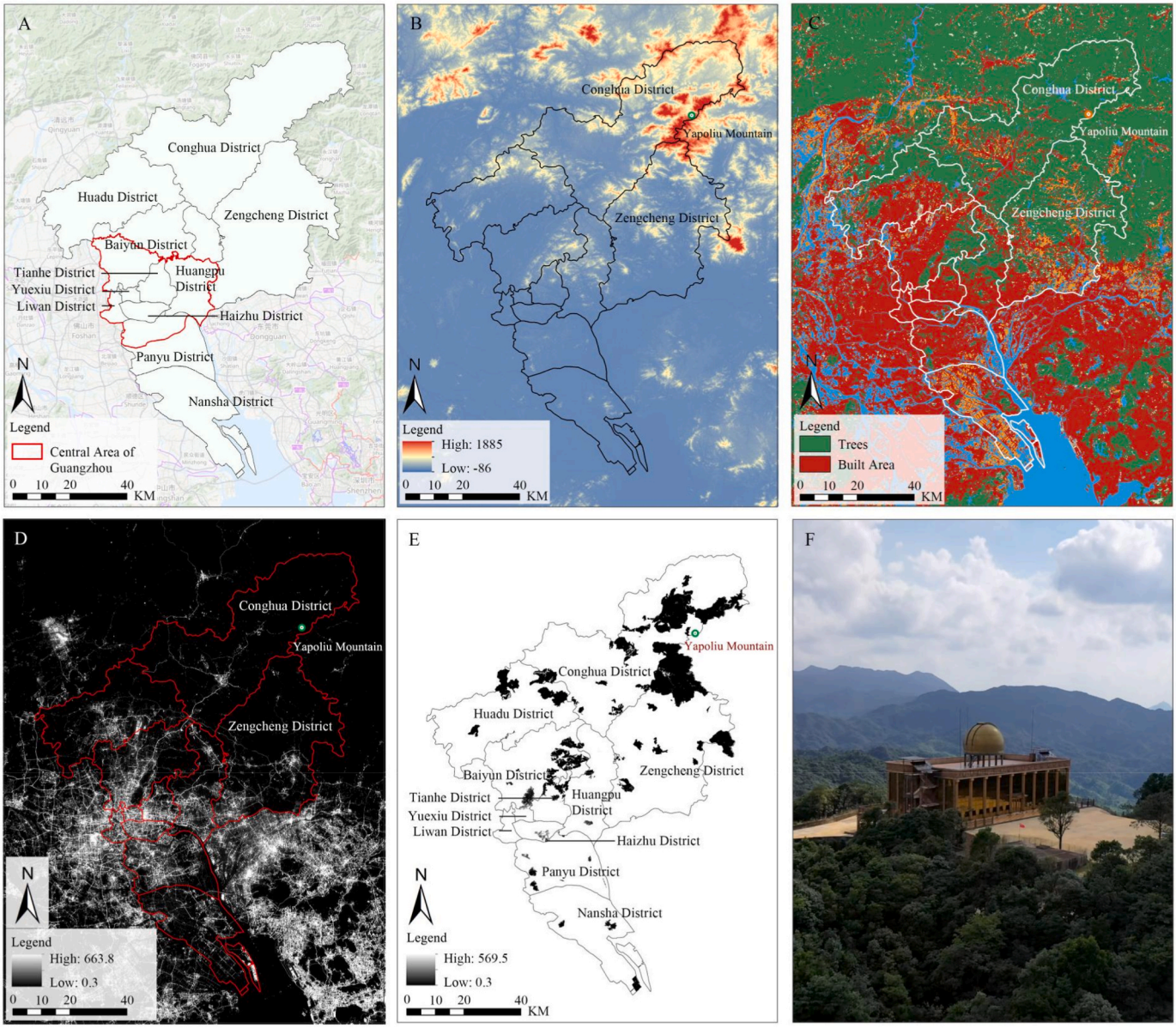

Fig. 1. Overview of the natural environment context of Guangzhou. (1-A Administrative divisions of Guangzhou; 1-B Digital elevation model of Guangzhou; 1-C Land cover map of Guangzhou; 1-D Light pollution map of Guangzhou; 1-E Light pollution map of nature protected areas in Guangzhou; 1-F Environmental context of the Yapoliu Mountain observation site in Conghua District).

2.2. Data sources and preprocessing

This study constructed a multidimensional dataset by integrating multi-source observational data from satellite and ground-based platforms, along with socio-economic geographic information. The primary data sources include nighttime light remote sensing data, in-situ zenith brightness measurements, all-sky fish-eye imagery, and basic geographic and socio-economic data.

(1) Satellite Remote Sensing Nighttime Light Data

SDGSAT-1-derived Nighttime Light Data: For the macro-scale analysis of light pollution characteristics, this study utilized SDGSAT-1 satellite nighttime light data provided by the International Research Center of Big Data for Sustainable Development Goals (CBAS). Operational since 2022, this dataset offers a high spatial resolution (10 m panchromatic and 40 m multispectral), enabling the fine-scale characterization of nighttime light patterns across urban areas and nature protected areas. A cloud-free image acquired on February 28, 2023, was selected for this research, with an acquisition time of approximately 21:30 (UTC+8) and a radiance range of 0.3–663.8 nW/(sr·cm^2). Preprocessing was conducted following the methodology of Liu et al. (2024), which included: (1) image denoising, involving stripe correction and salt-and-pepper noise removal; and (2) radiometric calibration, converting DN values to radiance using official calibration coefficients. This process generated a high-precision base map of light pollution distribution covering the entirety of Guangzhou, serving as the foundation for subsequent regional light environment background analysis.

Astronomy Outreach Light Pollution Map: To enable the rapid preliminary screening of light pollution conditions across all nature protected areas in Guangzhou, this study incorporated the Astronomy Outreach 2024 light pollution map dataset. This dataset is based on the radiative transfer model framework established in the World Atlas of Artificial Night Sky Brightness by Falchi et al. (2016), which enables the quantitative prediction of night sky brightness worldwide through atmospheric radiative transfer simulations. The core simulation principles

follow the light scattering and attenuation laws of the Garstang model and its extended versions. The primary input parameters include upward light flux data derived from satellite remote sensing, Digital Elevation Model (GTOPO30) terrain data, and regional atmospheric extinction coefficients.

In this study, the model was utilized to conduct a preliminary assessment of light pollution across 89 nature reserves in Guangzhou, aiming to rapidly identify candidate areas with relatively low light pollution levels to inform priority setting for subsequent ground-based verification using SQM measurements. It should be noted that estimates based on model simulations involve some degree of uncertainty. Nevertheless, at the macroscale, the model provides valuable insights into the gradient of light pollution in densely populated urban areas and supports the initial screening of dark sky resources across a wide range of nature reserves.

(2) Night Sky Quality Data

Based on the preliminary screening results and field verification, a ground observation site was established at the summit of Yapoliu Mountain in the northeastern part of Conghua District, Guangzhou. The site is situated at an elevation of approximately 730 m, atop a mountain range, offering an unobstructed view with no significant surrounding obstructions and located far from major urban light sources, thus providing favorable conditions for dark sky observations (Fig. 1-F). Two types of in-situ nighttime sky quality measurements were collected at this location:

SQM Zenith Brightness Data: Continuous fixed-point monitoring was conducted using an Unihedron Sky Quality Meter with Ethernet connectivity (SQM-LE). The observation window was scheduled from 19:00 daily to 06:00 the following day, with a sampling frequency of once per minute. The observation period spanned from December 2024 to June 2025. To ensure data quality, outliers resulting from extreme weather, high-brightness interference from the full moon, and periods of equipment signal interruption were excluded; this yielded 97 valid observation days and a cumulative total of 64,020 valid data entries.

All-Sky Fish-eye Imagery: An industrial camera (QHY600M, QHYCCD) equipped with a fish-eye lens was employed to capture full-dome night sky images for the identification of specific sources and azimuths of light pollution (Jechow et al., 2019). The camera sensor is a back-illuminated CMOS (IMX455) with a pixel size of 3.76 μm and an image resolution of 9600 × 6422 pixels (16-bit integer format). The lens is a Sigma 8 mm f/3.5 EX DG CIRCULAR FISHEYE, which features an equisolid-angle projection design. Observations were primarily concentrated on clear, moonless nights between December 2024 and February 2025, with a sampling interval of 10 min. The image resolution was 9600 × 6422 pixels (16-bit integer format), resulting in a total of 3960 valid images.

(3) Basic Geographic and Socio-economic Data

Auxiliary data utilized for site suitability evaluation and spatial correlation analysis primarily include:

Nature Protected Area Boundaries: Vector boundary data for 89 nature protected areas in Guangzhou, comprising forest parks, nature reserves, and wetland parks, were obtained from the Forestry Administration of Guangdong Province and subjected to topological verification and correction in accordance with the latest administrative divisions.

Digital Elevation Model (DEM) Data: Average elevation and slope data for the nature protected areas were derived from the Geospatial Data Cloud (https://www.gscloud.cn/). The SRTM 30 m resolution digital elevation model was utilized to analyze the topographic suitability for dark sky park site selection.

Land Use and Land Cover (LULC) Data: The 2024 forest cover data for Guangzhou were sourced from the ArcGIS Living Atlas of the World (https://livingatlas.arcgis.com/) at a spatial resolution of 10 m and applied in the analysis of topographic suitability for the selection of dark sky park sites.

Point of Interest (POI) Data: POI data regarding dining, accommodation, corporate enterprises, and public service facilities in Guangzhou for the year 2024 were acquired via the Amap Open Platform (https://lbs.amap.com/) to assess infrastructure maturity and analyze the perturbation of human activities on the luminous environment.

Traffic and Population Data: Transportation network data were derived from Open Street Map (https://www.openstreetmap.org/), while district-level demographic statistics were obtained from the *Communiqué of the Seventh National Population Census of Guangzhou*.

Tourism Resource Data: The directory and locational information of A-level tourist attractions were sourced from the Department of Culture and Tourism of Guangdong Province to evaluate proximity to scenic spots and the potential for industrial synergy.

3. Research methodology

This study adheres to a logical framework characterized by "macro-scale screening, micro-scale verification, and causal analysis". First, potential sites for dark sky parks are identified utilizing a multi-factor evaluation model; subsequently, the night sky quality of target areas is validated based on ground-based monitoring data; and finally, specific sources of light pollution are elucidated through multi-source data fusion techniques (Fig. 2).

3.1. Site suitability evaluation model for dark sky parks

To systematically identify potential dark sky park areas within the metropolitan fringe, this study developed an evaluation system consisting of six key indicators across three dimensions: environmental background, social disturbance, and service potential. First, utilizing 2024 light pollution map data, the study generated a light pollution intensity indicator (B1) via kernel density analysis and established multi-ring buffers to quantify the Euclidean distance between protected areas and the nearest town centers (B2), thereby characterizing the natural baseline of the dark sky environment. Second, considering the negative interference of human activities on the light environment, population density (B5) was calculated as the ratio of total population to land area; simultaneously, road network density (B3), POI facility density (B4), and proximity to A-level scenic spots (B6) were introduced as positive indicators to assess regional traffic accessibility and the potential for tourism service synergy.

For positive indicators (e.g., B2, B3, B4, and B6) and negative indicators (B5), Eqs. (1) and (2) were respectively applied to map the values onto a standardized interval. Subsequently, following the study by Chen et al. (2023) regarding the weighting of site selection indicators for dark sky parks, the Analytic Hierarchy Process (AHP) was utilized to construct a judgment matrix. After passing the consistency test, the weights for each indicator were determined (Table 1). Finally, the Dark Sky Park Construction Suitability Comprehensive Evaluation Index (DSPCFI) was established through weighted overlay (Eq. (3)). This model is designed to screen and identify the regions with the highest composite scores as the primary subjects of investigation.

$$y_{+} = \frac{x - x_{min}}{x_{max} - x_{min}} \tag{1}$$

$$y_{-} = \frac{x_{max} - x}{x_{max} - x_{min}} \tag{2}$$

$$DSPCFI = \sum_{i=1}^{6} (W_i \times B_i) \tag{3}$$

In the formula, W_i represents the weight of the i-th indicator, and B_i

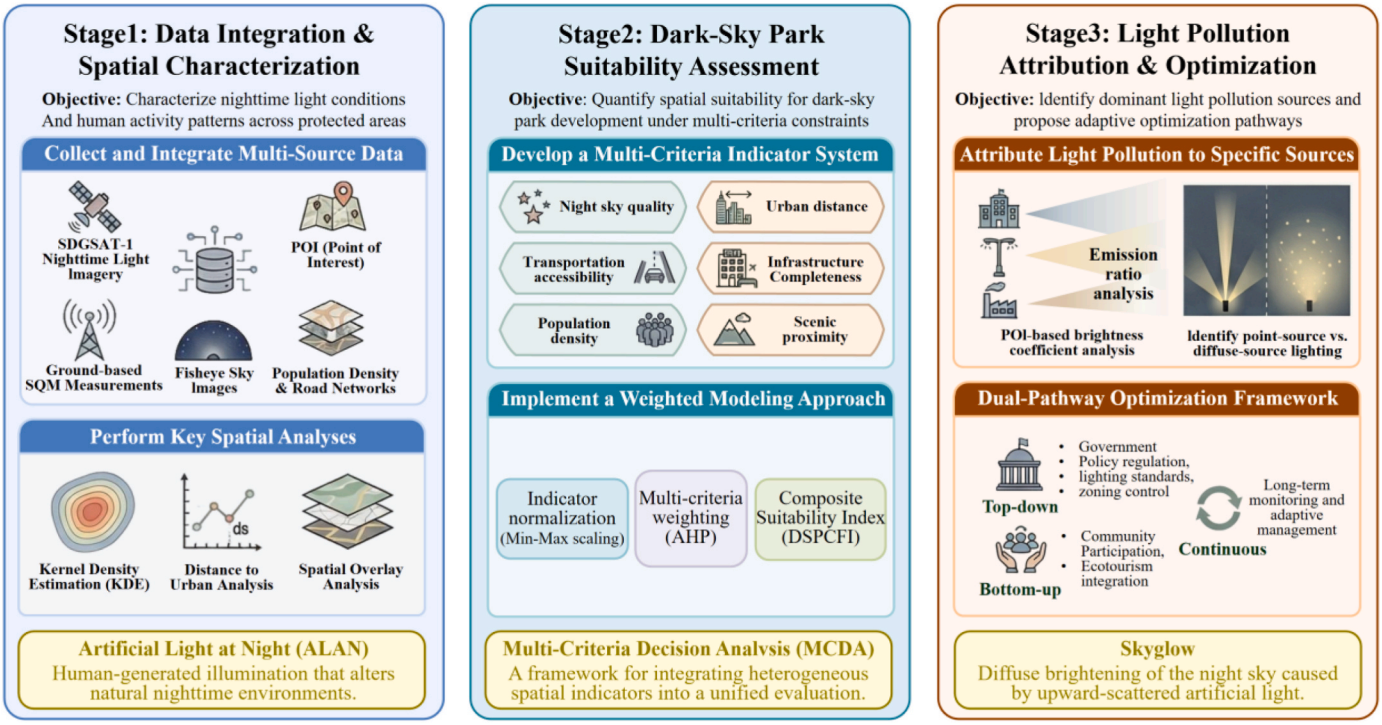

Fig. 2. Research framework and technical roadmap.

Table 1
Indicator system and weighting for dark sky park siting suitability assessment.

Objective A	Criterion B	Weight
A1. Comprehensive suitability assessment for establishing a dark sky park	B1. Night sky quality	0.3488
	B2. Urban distance	0.1532
	B3. Transportation accessibility	0.0835
	B4. Infrastructure completeness	0.0519
	B5. Population density	0.1346
	B6. Scenic proximity	0.2280

denotes the standardized value of the indicator.

3.2. Ground-based night sky quality observation and data inversion

To validate the accuracy of the macro-scale site selection model and obtain high-precision light environment parameters, this study utilized SQM-LE and all-sky fish-eye cameras as ground-based monitoring equipment to continuously observe night sky quality, cross-referencing the observational results from both instruments.

Raw camera images underwent preprocessing, including denoising and background subtraction, using MaxIm DL 6 software to obtain net signal values, after which they were imported into ds9 software for visualization (Joye and Mandel, 2003). The conversion of pixel grayscale values into standard magnitude values involved two stages: (1) Calibration of the instrumental conversion parameter Z_0: Zenith brightness values consistent with the imaging time of the fish-eye images were selected from the SQM ground-based measurements, denoted as M_{SQM} (mag/arcsec^2). Simultaneously, the preprocessed average grayscale value of the central zenith region (300 × 300 pixels) of the fish-eye image was extracted and substituted into Eq. (4) to inversely solve for Z_0; (2) Calculation of M_{SKY}:Using the calibrated Z_0, the brightness value M_{SKY} at any position across the entire sky was calculated using Eq. (5). This enabled a reliable analysis of night sky brightness and the spatial distribution of terrestrial light pollution sources.

$$M_{SQM} = 25 - 2.5\lg\left(\frac{ADUs}{T \times scale^2}\right) + Z_0 \tag{4}$$

$$M_{SKY} = 25 - 2.5\lg\left(\frac{ADUs}{T \times scale^2}\right) + Z_0 \tag{5}$$

In the formula, M represents the night sky brightness (mag/arcsec^2), Z_0 is the instrumental zero-point constant, $ADUs$ denotes the preprocessed grayscale value of the pixel, T indicates the exposure time (20 s), and $scale$ refers to the pixel scale (115″/pixel).

Determination of the Pixel Scale: Based on the equisolid-angle projection model of the fisheye lens (f = 8 mm, pixel size = 3.76 μm; Eq. (6)), the differential relationship (Eq. (7)) was employed to calculate the instantaneous pixel scale at different radial positions (Eq. (8)). A curve showing the variation of the pixel scale with radial distance R (pixels) was subsequently plotted. Calculations indicated that within the effective imaging range (maximum radial distance of 3134 pixels), the variation in scale was limited. To simplify the zenith brightness calculation, the median pixel scale of the entire image was adopted as a constant, namely 115"/pixel. Verification work on 8 mm fish-eye lenses by Schneider et al. (2009) also demonstrated that following radial distortion correction, different projection models can achieve sub-pixel measurement accuracy, providing theoretical support for the use of a constant scale approximation.

$$R = 2f\sin\frac{\theta}{2} \tag{6}$$

$$\frac{d\theta}{dr} = \frac{2}{\sqrt{4f^2 - r^2}} \tag{7}$$

$$r = R \times 3.76\mu m \tag{8}$$

3.3. Light pollution source tracing analysis based on POI data

To precisely pinpoint specific pollution sources within and surrounding protected areas, this study employs multi-source data fusion

techniques to analyze the spatial correlation between Points of Interest (POI) and nighttime light intensity. By overlaying SDGSAT-1 remote sensing imagery with classified POI data encompassing six categories, including commercial facilities, corporate enterprises, public services, road transportation, and accommodation services, the brightness coefficient (l_j) and luminosity proportion (p_j) for each facility type were calculated (Tang et al., 2020). The brightness coefficient serves to quantify the average luminous intensity of a single facility category (Eqs. (9) and (10)), whereas the luminosity proportion is utilized to assess the contribution weight of that category to the total regional light radiance (Eq. (11)).

$$k_i = \frac{Brightness_i}{\frac{1}{n}\sum_{k=1}^{n} Brightness_k} \tag{9}$$

$$l_j = \frac{1}{m_j}\sum_{i=1}^{m_j} k_i \tag{10}$$

$$p_j = \frac{\sum_{i=1}^{m_j} Brightness_i}{\sum_{k=1}^{6} Brightness_k^*} \tag{11}$$

In the formulas, k_i represents the brightness coefficient of the i-th point, and $Brightness_i$ denotes the radiance of the remote sensing pixel corresponding to the i-th POI. n is the total number of pixels in the study area. l_j is the average brightness coefficient of the j-th POI category, and m_j denotes the number of pixels in that category; p_j represents the luminosity proportion of the j-th POI category; $Brightness_j^*$ defined as the aggregate brightness (total radiance) of all pixels within that category. To avoid ambiguity, distinct symbols (i, j, and k) are used to denote POI indices, category indices, and dummy indices in summations, respectively.

Based on the aforementioned indicators, this study further established multi-level gradient buffers centered on the protected areas, spanning radii of 2 km (boundary zone), 6 km (buffer zone), and 10 km (peripheral zone). The 2 km boundary zone is defined as the core near-field space where protected areas are subject to direct anthropogenic interference (Newbold et al., 2015). The 6 km buffer zone serves as a gradient transition interval where near-field direct interference shifts toward far-field indirect interference (Jiang et al., 2026). Finally, 10 km represents the sensitive distance for the response of nature protected areas to the intensity of human activities (Jiang et al., 2022). By comparing the characteristics of brightness coefficients and luminosity proportions of various POIs across different distance zones, this approach distinguishes between high-brightness point sources (e.g., individual high-intensity lighting facilities) and low-brightness area sources (e.g., urban agglomerations). It also reveals the gradient interference effects of transportation corridors and village activities on the light environment of protected areas, thereby providing a quantitative basis for differentiated management strategies.

4. Results and analysis

4.1. Identification results of candidate sites for dark sky parks

A total of 13 nature protected areas in Guangzhou satisfy the screening benchmark of SQM ≥20.5 mag/arcsec^2; these sites are concentrated in the northeastern Conghua and Zengcheng Districts, regions characterized by superior ecological background conditions (Fig. 3-A). Among these, Dark sky zones meeting the Dark-Sky International (IDA) Silver Tier standard (21.00–21.74 mag/arcsec^2) are significantly scarcer, comprising only six protected areas situated exclusively in the northeastern sector of Conghua District.

A spatial analysis of the various suitability conditions for candidate protected areas revealed the following results: regarding distance from town centers (Fig. 3-D), protected areas within Lütian and Liangkou Towns in Conghua District are furthest, approximately 40 to 50 km away, thereby experiencing minimal interference from artificial lighting; in terms of traffic accessibility (Fig. 3-E), the road network density within protected areas in Liangkou Town is relatively high, with roads encircling or traversing the sites to ensure good external connectivity and facilitate public access; regarding the maturity of tourism infrastructure (Fig. 3-F), dining and accommodation facilities are most densely distributed around Wuzhishan District-level Forest Park and Lianxi Municipal Forest Park, forming a substantial tourism service system capable of supporting the subsequent operation of dark sky parks; concerning population density (Fig. 3-G), Lütian and Liangkou Towns record densities of 61 persons/km^2 and 71 persons/km^2, respectively, marking them as sparsely populated areas where low human activity intensity creates favorable conditions for light pollution control; and regarding proximity to scenic spots (Fig. 3-H), the high concentration of attractions surrounding Liuxi River National Forest Park and Shimen National Forest Park demonstrates strong potential for the synergistic and coordinated development of tourism resources.

Synthesizing the multi-dimensional evaluation results, the sites suitable for the construction of dark sky parks in Guangzhou are primarily concentrated in Liangkou Town, Conghua District (Fig. 3-B). The specific comprehensive evaluation scores and rankings for each protected area are presented in Table 2; notably, Guangzhou Conghua Lianxi Municipal Forest Park ranks first with a composite score of 0.89, exhibiting significant advantages in dark sky environmental quality, locational conditions, traffic accessibility, and service infrastructure, making it the optimal site for establishing a dark sky park in Guangzhou. Based on DEM data analysis, Lianxi Municipal Forest Park exhibits an average elevation of 661 m; this high altitude is conducive to shielding the area from external residential light sources. The terrain is moderately steep, with an average slope of 20.2°, yet it remains accessible for pedestrian ascent. Furthermore, the established internal road network within the park facilitates vehicular access. While vegetation in South China is typically tall and dense, which often obstructs celestial observations, Lianxi's vegetation coverage rate of 88.6% is relatively low among the selected protected areas. This preserves sufficient open spaces suitable for dark sky activities such as stargazing and camping.

Following closely are Zhengguo Lake Central Island Wetland Park in Zengcheng District and Liuxi River National Forest Park, which achieved nearly identical scores of 0.83 and 0.82, respectively. Despite its high ranking, Central Island Wetland Park is situated at an elevation of only 15 m with flat terrain; combined with a low vegetation coverage rate of 28.9%, it is highly susceptible to the intrusion of light pollution from surrounding areas. In contrast, Liuxi River National Forest Park features an average elevation of 400 m, an average slope of 18.5%, and a vegetation coverage rate of 79%. Its superior overall topographic conditions render it a viable alternative site for dark sky park construction.

4.2. Night sky quality Monitoring Results

(1) SQM-LE Monitoring Results

Statistical analysis of the valid zenith brightness data yielded a mean of 19.3 mag/arcsec^2, a median of 20.1 mag/arcsec^2, a standard deviation of 2.3 mag/arcsec^2, a minimum of 5.9 mag/arcsec^2, and a maximum of 21.28 mag/arcsec^2. Notably, the minimum value is significantly lower than natural night sky brightness, likely due to interference from moonlight, twilight, or local artificial light sources. To focus on the intrinsic night sky quality baseline, Fig. 4-A presents the histogram of zenith brightness distribution derived from observational samples where the brightness was no less than 15 mag/arcsec^2. The figure indicates that the peak zenith brightness is 20.4 mag/arcsec^2, with a frequency reaching 6,000, suggesting that this brightness level represents the prevailing condition of the local night sky. To verify the robustness of the data distribution, a normalization process was applied (excluding

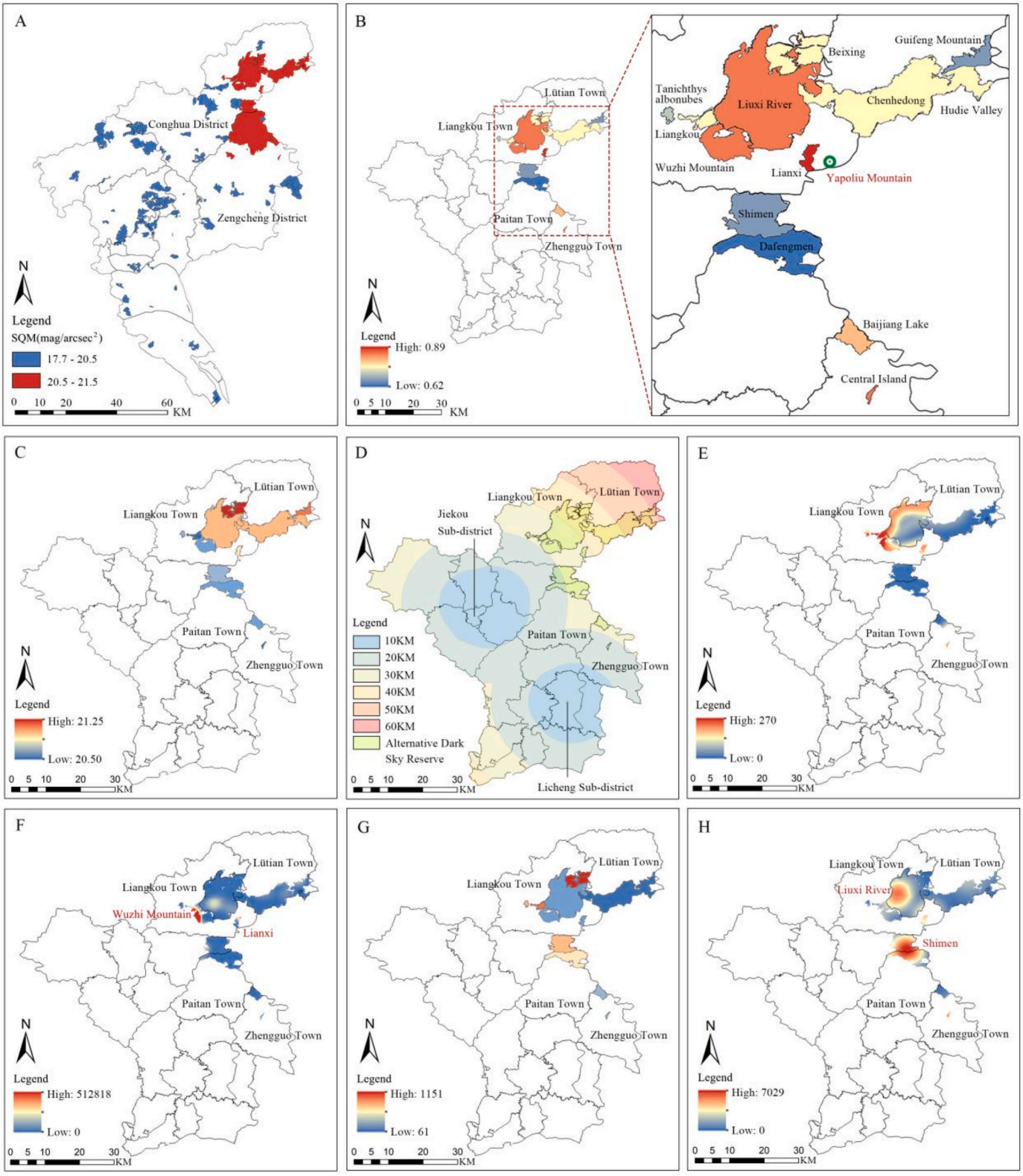

Fig. 3. Suitability assessment maps for site selection. (3-A Spatial distribution of nature protected areas with $SQM \geq 20.5$ in Guangzhou; 3-B Comprehensive suitability evaluation results for dark sky park site selection in candidate protected areas; 3-C Night sky quality analysis of candidate protected areas; 3-D Analysis of distance between candidate protected areas and towns; 3-E Analysis of transportation accessibility of candidate protected areas; 3-F Analysis of infrastructure completeness of candidate protected areas; 3-G Analysis of population density of candidate protected areas; 3-H Analysis of scenic spot proximity of candidate protected areas).

Table 2
Statistical table of suitability assessment for dark sky parks in candidate protected areas.

Rank	Score	Protected Areas	Abbr.	Average Elevation (m)	Average Slope (°)	Vegetation Coverage Rate (%)
1	0.89	Guangzhou Conghua Lianxi Municipal Forest Park	Lianxi	661	20.2	88.6
2	0.83	Zengcheng District Zhengguo Lake Central Island Wetland Park	Central Island	15	3.6	28.9
3	0.82	Guangdong Liuxi River National Forest Park	Liuxi River	400	18.5	79.0
4	0.81	Guangzhou Conghua Wuzhi Mountain District-level Forest Park	Wuzhi Mountain	593	25.2	99.2
5	0.75	Guangzhou Baijiang Lake Forest Park	Baijiang Lake	267	19.2	98.8
6	0.72	Guangdong Conghua Chenhedong Provincial Nature Reserve	Chenhedong	547	21.3	94.3
7	0.72	Guangzhou Conghua Liangkou District-level Forest Park	Liangkou	150	19.5	93.9
8	0.71	Guangzhou Conghua Beixing District-level Forest Park	Beixing	268	16.5	98.7
9	0.68	Guangzhou Conghua *Tanichthys albonubes* Municipal Nature Reserve	*Tanichthys albonubes*	203	13.3	100
10	0.66	Guangdong Shimen National Forest Park	Shimen	661	22.5	95.2
11	0.66	Guangzhou Conghua Guifeng Mountain Ancient Human Site District-level Forest Park	Guifeng Mountain	549	25.1	96.9
12	0.65	Guangzhou Conghua Hudie Valley District-level Forest Park	Hudie Valley	534	22.1	99.2
13	0.62	Guangzhou Dafengmen Forest Park	Dafengmen	682	22.7	97.4

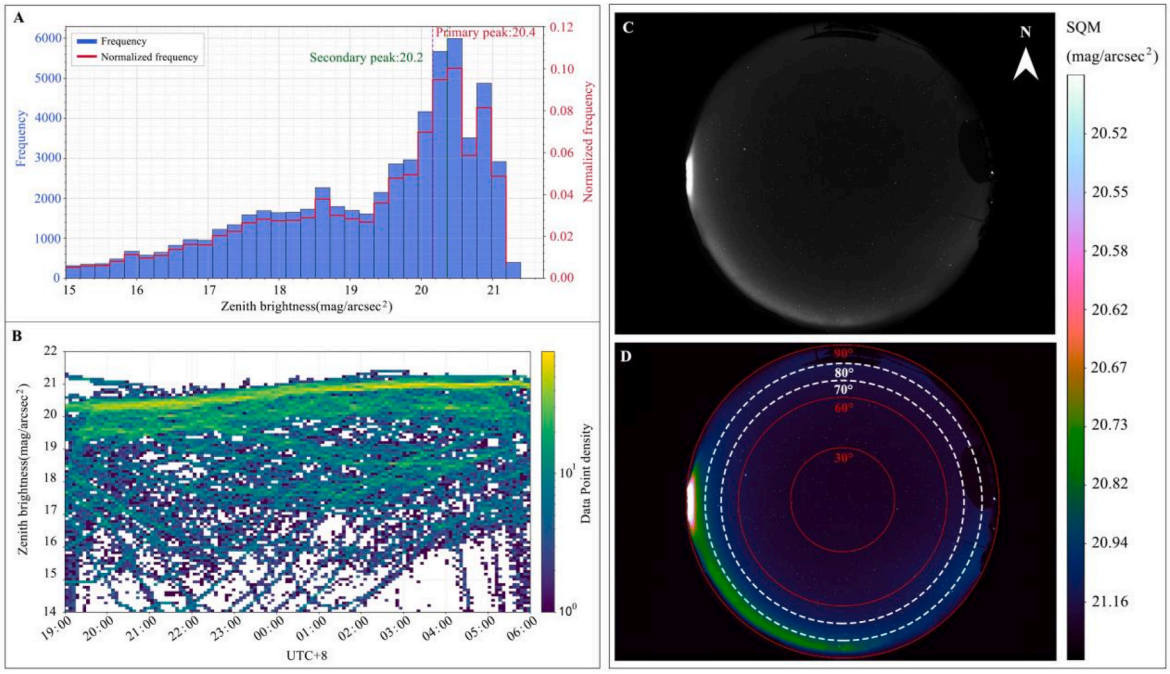

Fig. 4. Ground-based measurement analysis at Yapoliu Mountain. (4-A Zenith brightness histogram, SQM≥15; 4-B Zenith brightness-frequency distribution density plot; 4-C Raw fish-eye image; 4-D Pseudo-color processed fish-eye image).

samples with night sky brightness lower than 15 mag/arcsec^2); the results reveal that the main peak remained stable at 20.4 mag/arcsec^2, with the vast majority of observations distributed within the 19.5–21.2 mag/arcsec^2 range. This indicates that Lianxi Forest Park already possesses the requisite night sky quality baseline for designation as an International Dark Sky Park. In the future, through scientific lighting controls and regional collaboration, its night sky quality is expected to improve further, potentially reaching the Silver Tier ($21.00 \leq SQM \leq 21.74$) or higher standards (International Dark-Sky Association, 2018).

The night light-frequency distribution density plot (Fig. 4-B) further reveals that starting from 20:00, the night sky quality reaches a relatively ideal level, with SQM values remaining stable at or above 20 mag/arcsec^2 (as indicated by the yellow line). During this period, a star-filled sky is clearly visible, and the quality continues to enhance as the night progresses. The post-midnight period (02:00-05:00) offers the most ideal conditions, where SQM values can reach 21 mag/arcsec^2 or higher, representing the optimal window for astronomical observation.

(2) Distribution Characteristics of All-Sky Night Sky Brightness

The fish-eye image presented in Fig. 4-C was captured at 05:00 on January 4, 2025, and underwent contrast enhancement processing. Weather conditions on that day were favorable, characterized by the absence of moonlight and cloud interference. The measured zenith brightness reached 21.28 mag/arcsec^2. Fig. 4-D illustrates a pseudo-color image generated within the brightness range of 20.51–21.16 mag/arcsec^2, which was utilized to analyze brightness gradations across the full celestial dome and within various zenith angle intervals, as well as to determine the spatial distribution of terrestrial light sources. The imagery reveals that the darkest region is within 60 degrees of the zenith angle; the brighter regions of the sky are distributed within the zenith angle range of 70° to 90°, with the highest concentration occurring in the 80° to 90° interval. Specifically, the area approximately 10° above the horizon is most significantly impacted by ALAN. The bright white arc situated due west constitutes the brightest region of the entire sky, exhibiting a brightness of approximately 20 mag/arcsec^2. The night sky brightness in this region is primarily attributed to vehicular traffic and street lighting on the Shanzhan Expressway, located approximately 2.5 km west of the observation point. A green luminous arc is observable in

the southwest direction, with a brightness of approximately 20.8 mag/arcsec^2. Integrating the analysis of satellite remote sensing light distribution and POI data, it is inferred that the sky brightness here is influenced by Jiekou Subdistrict in Conghua District, located 30 km away; conversely, the area south of the observation point is Nankunshan Forest Park, and the remaining regions are predominantly covered by forest vegetation, exhibiting relatively low levels of light pollution.

4.3. Analysis Results of Light Pollution Sources Based on POI and field surveys

(1) Analysis Results of Light Pollution Sources Based on POI Data

By calculating the quantity of POIs in each buffer zone, the brightness coefficient (the ratio of the average brightness value of a specific POI category to the average brightness value of all POIs, characterizing the unit brightness level), and the luminosity proportion (the ratio of the total brightness value of a specific POI category to the total brightness value of all POIs, quantifying the contribution to overall light pollution), the following results were obtained.

Spatial gradient distribution characteristics of total POI quantity: The total number of POIs exhibits a clear gradient increase as the buffer zone expands (Fig. 5-A, Table 3). The number of POIs is only 21 within the protected area, which increases to 213 within the 2 km buffer, reaches 340 within the 6 km buffer, and rises as high as 694 within the 10 km buffer. This distribution pattern reflects the spatial differentiation characteristic wherein the intensity of human activity gradually increases from the core area of the protected land toward the periphery; this aligns highly with the strict development control policies within the protected area and the reality of continuous expansion of human activity in the peripheral regions.

Characteristics of light pollution sources within the protected area: Although the overall quantity of POIs within the protected area is low, public service facilities (including campsites, service stations, and farmhouses) exhibit a significant "low quantity-high intensity" characteristic; with a brightness coefficient 4-5 times the average level of all POIs, they constitute the primary high-brightness point sources internally, exerting a direct and significant interference on the nocturnal light environment of the core area.

Differences in light pollution characteristics across different buffer zones: The structures of brightness coefficients and luminosity proportions for POIs within the 2 km and 6 km buffer zones are highly

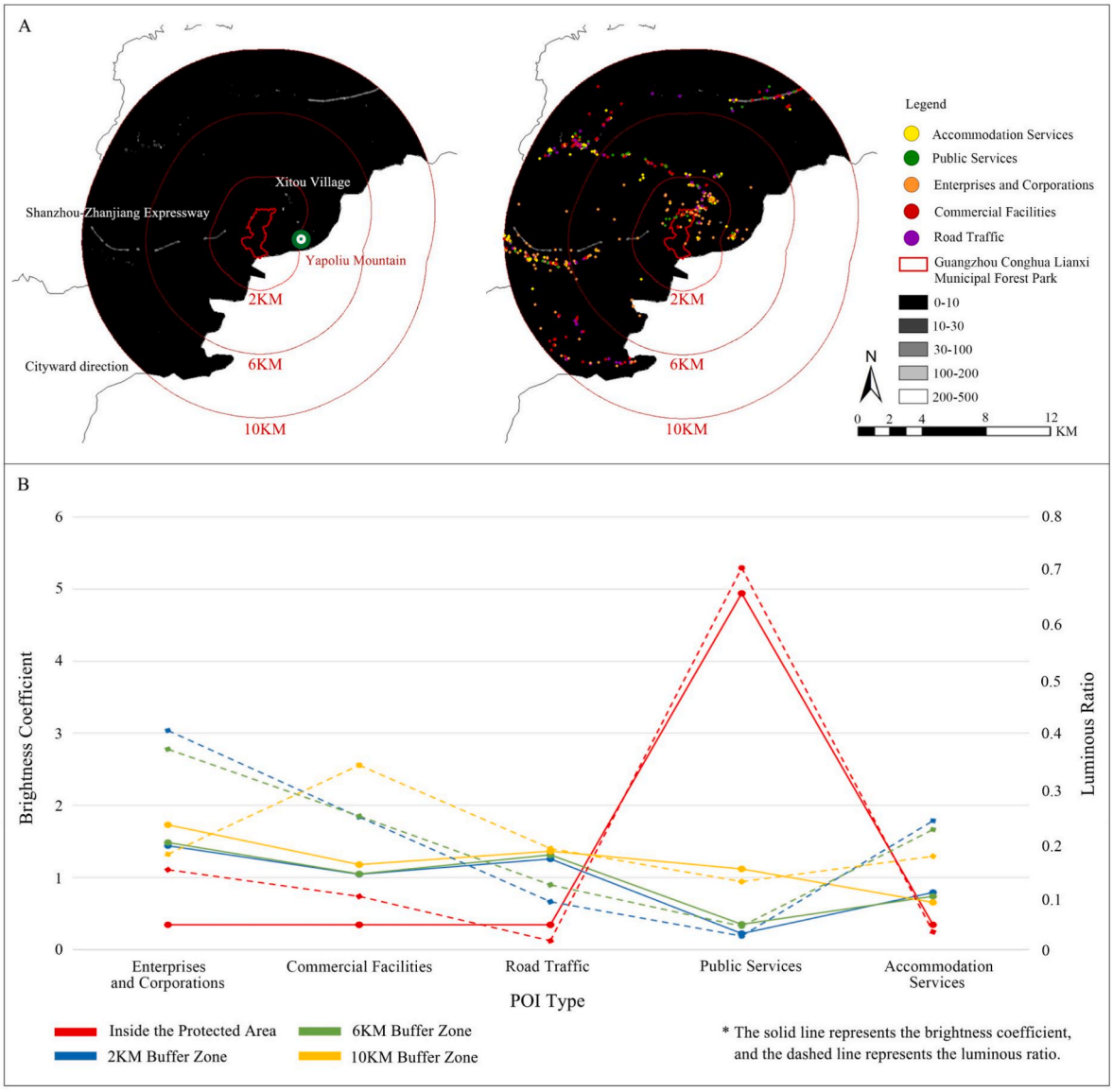

Fig. 5. Light pollution analysis map of Lianxi Municipal Forest Park. (5-A POI distribution map; 5-B Analysis of POI brightness coefficient and luminous proportion).

Table 3
Statistical table of POI quantity in Lianxi Municipal Forest Park.

	Accommodation Services	Public Services	Enterprises and Corporations	Commercial Facilities	Road Traffic
Alternative Dark Sky Reserve	2	3	9	6	1
2 km	64	24	60	50	15
6 km	102	42	85	80	31
10 km	183	78	137	201	95

similar (Fig. 5-B); specifically, the brightness coefficients for various POI categories remain stable within the average range, and the distribution patterns of luminosity proportions tend to be consistent, indicating that human activity intensity and lighting levels exhibit a uniform expansion trend within this distance range without significant abrupt changes in characteristics. When the buffer zone range expands from 6 to 10 km, distinct differences appear in light environment characteristics, manifested by an increase in the brightness coefficient of commercial facilities and a significant reconfiguration of luminosity proportions across POI categories. This indicates the intervention of high-intensity socio-economic activities from main urban functional zones, such as the Conghua central area, which come to dominate the light environment pattern of the region.

Light pollution effects of different POI types: ① High-intensity point sources generate localized intense light pollution. Although public service facilities generally have a low luminosity proportion, the intensity of localized ecological interference they generate may far exceed the levels reflected by their luminosity proportions, posing a potential threat to the stability of the nocturnal environment of ecosystems within the protected area. ② Medium-to-low brightness area sources generate a cumulative pollution effect. Within the 2 km and 6 km buffer zones, the brightness coefficients of corporate enterprise POIs are generally at a medium-to-low level, however, the luminosity proportion of this category remains consistently high, reflecting the cumulative light pollution effect resulting from their large distribution quantity. Commercial facilities within the 10 km buffer zone exhibit similar characteristics, namely that while unit brightness is not high, the total pollution contribution is significant. Furthermore, the impact of transportation facilities cannot be overlooked.

(2) Field Survey Results of Lighting Facilities

On November 22–23, 2025, a field survey of light sources was conducted at Liuxi River National Forest Park and Lianxi Municipal Forest Park. Seven categories of light sources were identified in Liuxi River National Forest Park, distributed primarily near the park entrance, visitor center, roadways, hotels, and restrooms (Table 4). An OHSP-350 hand-held spectral color illuminance meter was employed to measure the light sources. Measurements were conducted at a horizontal distance of 1 m from the source and a vertical height of 1.5 m above the ground, with the peak values recorded. The results indicated that the illuminance of the various light sources ranged from 2.88 lx to 70.80 lx. Notably, the LED lighting at the park entrance exhibited a brightness as high as 70.80 lx—approximately 6.4 times that of the park's streetlights—constituting the highest-intensity point source of interference in the area. Streetlights were the most numerous and widely distributed source, spaced approximately 15 m apart with a total count of around 350, and were scheduled to be extinguished daily at 22:30. On the night of observation, zenith brightness at both monitoring sites decreased significantly following the extinguishment of the streetlights. Specifically, the night sky brightness at the Science Popularization Plaza shifted from 20.28 to 20.52 mag/arcsec^2, while at the Forest Campsite monitoring point, it improved from 20.45 to 20.58 mag/arcsec^2 (Fig. 6). These results indicate that street lighting significantly affects night-sky brightness within the park.

With the exception of surveillance lights at the visitor center, luminaires within the park exhibit color temperatures exceeding 4500 K. These fixtures function as white light sources with a predominant blue wavelength component, indicating that they are not dark-sky-friendly.

Table 4
Lighting fixture inventory at Liuxi River Forest Park.

No.	Name	Illuminance (lx)	Color Temperature (K)	Spectrum	Luminaire Photos	Shielded or not	Light Source Color
1	Street Light at the Park Gate	5.40	6307			Partially Shielded	White
2	LED Light at the Park Gate	70.80	5632	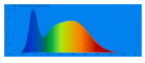		Unshielded	White
3	Entrance Street Light	2.88	4599	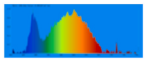		Unshielded	White
4	Campus Light	11.10	4620	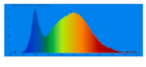		Partially Shielded	White
5	Restroom Light	7.54	6647	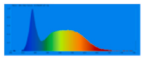		Partially Shielded	White
6	Surveillance Light at the Visitor Center	3.65	2984	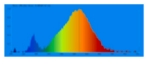		Unshielded	Orange
7	Hotel Street Light	5.08	5503			Shielded	White

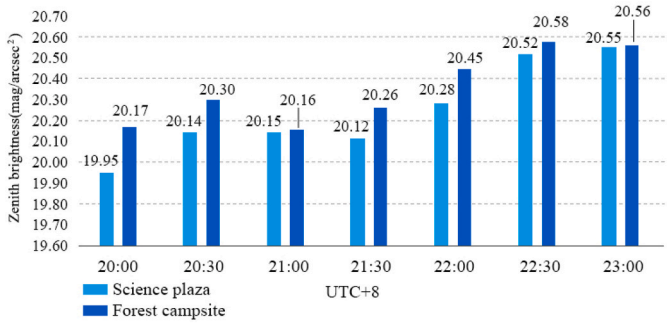

Fig. 6. Zenith brightness at two observation sites in Liuxi River Forest Park.

With respect to shielding status, the majority of fixtures in the park are either unshielded or partially shielded, allowing light to be emitted directly toward the sky and thereby generating significant upward luminous flux. This constitutes a critical area requiring remediation in the context of establishing a dark sky park.

In contrast to Liuxi River National Forest Park, Lianxi Municipal Forest Park possesses fewer internal light sources; although streetlights and camping facilities are present at the entrance, they remained unilluminated during the night of the survey.

5. Discussion

5.1. The uniqueness and urgency of dark sky conservation in the urban fringe of megacities

Historically, global practices in dark sky conservation have predominantly focused on pristine dark skies located in high plateaus or deserts far from human settlements. However, this study identifies high-quality dark sky patches, exemplified by Lianxi Forest Park, on the periphery of Guangzhou, a megacity with a population approaching twenty million, challenging the conventional assumption that dark sky parks cannot be established in high-density cities. Such "dark sky enclaves" situated on the fringes of megacities possess social values unmatched by traditional wilderness protected areas: located within the "1-h commuting circle" of major urban centers, they dismantle the geographical barriers that restrict premium starry sky resources to a minority of professional enthusiasts, thereby realizing "public sharing" and "opportunity equity" of dark sky resources. The existence of areas such as Lianxi in Conghua confirms that, through the combined action of natural terrain barriers like mountain ranges and low light pollution levels, megacities are fully capable of preserving high-quality dark sky baselines within the "urban-nature" transition zone. This scarce "near-city dark sky resource" serves not only as a unique hallmark of urban ecological civilization construction but also as a valuable asset for psychological healing and nature education for high-stress urban populations.

Unlike the relatively simple background night sky environments in remote inland regions, dark sky conservation in urban fringe areas must address a complex and heterogeneous environmental substrate. Multi-source data analysis in this study reveals that this region constitutes a zone of intense conflict between high-intensity ALAN and the natural dark sky. Coupled analysis using SDGSAT-1 remote sensing and fish-eye imagery demonstrates that the light environment of the target area exhibits extreme spatial heterogeneity: it must simultaneously withstand lateral light intrusion from linear infrastructure such as the Shanzhan Expressway and cope with area-source skyglow interference from the Conghua central district. This complex "source-sink" landscape pattern implies that the dark sky environment in the urban fringe is extremely fragile; rather than a stable natural baseline, it represents an "ecological island" highly susceptible to being engulfed by external waves of light. Consequently, its conservation possesses heightened urgency, whether viewed from the perspective of astronomical observation or ecological protection.

Based on the POI source tracing analysis results of this study, within the 6 to 10 km periphery of the protected areas, the luminosity proportion of commercial and corporate facilities has assumed a dominant position and exhibits a significant trend of cumulative growth. This outside-in "light pollution siege" effect continuously erodes the night-sky quality of the core area in the form of diffuse skyglow (Jechow et al., 2017; Kocifaj et al., 2024). Given that northern Guangzhou is currently in an accelerating phase of rural revitalization and tourism development, failure to establish strict dark sky protection mechanisms within this window of opportunity could result in the complete disappearance of these remaining dark sky patches within the next 5 to 10 years due to urban sprawl (Jiang et al., 2018). Therefore, implementing dark sky conservation on the fringes of megacities is not merely an aesthetic enhancement, but a salvage operation racing against disorderly urban expansion.

5.2. Hierarchical zoned management strategies based on multi-source data attribution

The analysis of POI brightness coefficients reveals that within the protected area, despite a low total volume of POIs, public service facilities exhibit brightness coefficients significantly exceeding the average level, thereby displaying typical characteristics of "high-intensity point sources". Field research further confirms that LED lighting at the park entrance reaches an illuminance as high as 70.80 lx, with a significant proportion of blue light in its spectrum, which adversely impacts astronomical observations (Bará, S., & Bao-Varela, 2023). This result indicates that the paramount objective within the core area is not the comprehensive reduction of human activity, but rather the precise management and control of a minority of "super-emitters". Therefore, it is recommended to designate the protected area as a "Dark Sky Core Conservation Zone". Within this zone, management strategies should specifically target these high-coefficient facilities by mandating a reduction in the lighting intensity of relevant public service infrastructure to less than 50% of current levels (thereby eliminating abnormal outliers). While Dark-Sky International regulations stipulate that the Correlated Color Temperature (CCT) in core areas should be limited to below 3000 K, this threshold remains relatively high for ecologically sensitive regions. Based on measured color temperature data, the use of blue-rich light sources with a CCT exceeding 2200 K should be strictly prohibited (Dalgleish, 2021; Hung et al., 2021; Labrousse et al., 2025) to intercept the direct intrusion of high-intensity point sources into the core ecological zone. Furthermore, in habitats for fireflies and other nocturnal species, the use of lighting facilities must be completely restricted, as the presence or absence of light—rather than its spectral composition—is the most fundamental factor impacting the ecosystem (Robert et al., 2025).

As the distance extends to the 6 km buffer zone, the driving mechanism of light pollution undergoes a fundamental shift: although the brightness coefficient of individual enterprises regresses to the average range, their luminosity proportion rises significantly due to a surge in quantity, resulting in a "cumulative effect of low-brightness area sources" that is difficult to mitigate through single-point governance. This abrupt characteristic transition provides a distinct spatial basis for the delineation of a "Buffer Control Zone". To address the region's characteristic of being "widely distributed, with low individual brightness but high aggregate brightness", management strategies must shift from "individual fixture control" to "regional total quantity control". It is recommended that strict limits be imposed on the total lighting power density for enterprise-designated land at the planning approval level to prevent the disorderly sprawl of low-brightness area sources; this approach aims to achieve an 80% reduction in regional light emissions by controlling the accumulation of total luminous flux (Bará et al., 2021; Falchi and Bará, 2020).

Regarding the peripheral area spanning 6 to 10 km, all-sky fish-eye imagery precisely captured urban skyglow emanating from the direction of the Conghua central district, confirming that peripheral commercial facilities constitute the primary source of interference. Mere static zoning is insufficient to address this challenge. Therefore, dynamic technical measures are proposed within a "Peripheral Collaborative Governance Zone". Dark sky conservation indicators should be incorporated into commercial land planning guidelines for this region to mitigate external high-intensity light interference at the macro-spatial level by directing high-intensity commercial activities away from the protected area. Simultaneously, emphasis should be placed on promoting Adaptive Lighting Systems for identified major transportation arteries; these systems dynamically adjust brightness based on traffic flow and moonlight conditions, thereby attenuating the radiant intensity of linear light bands at the source (Gagliardi et al., 2020; Shavkatov, 2023).

5.3. Limitations and future prospects

While this study has validated the efficacy of the site selection model through the fusion of multi-source data, certain limitations remain regarding the temporal coverage of the dataset. The in-situ ground-based SQM measurement data primarily spans the period from December 2024 to June 2025, resulting in a deficit of continuous observational samples for the summer and autumn seasons. This constraint is predominantly attributable to Guangzhou's subtropical monsoon climate, characterized by high precipitation and extensive cloud cover during the summer, which objectively restricts the window for effective astronomical observation. Although the existing data encompass the region's primary "clear and dry window", which is sufficient to substantiate the feasibility of establishing a dark sky park, the nuanced impacts of annual meteorological conditions—such as the amplification of urban skyglow due to cloud reflection effects—on night sky quality remain to be elucidated through longer-term monitoring.

Regarding the construction of the site suitability evaluation model, this study currently prioritizes physical and socio-economic indicators related to "optical environmental quality" and "construction feasibility". However, for a dark sky park where ecological conservation is paramount, the model has not yet fully incorporated indicators of "ecological sensitivity" (Das et al., 2025; Vardi-Naim et al., 2022), such as the distribution ranges of keystone nocturnal species and migration corridors. This implies that while the currently selected optimal sites (e.g., Lianxi Forest Park) possess the superior light environments and most comprehensive supporting facilities, further verification is required to determine whether they constitute the most critical areas for biodiversity conservation. The spatial coupling relationship between physical suitability and ecological urgency represents a pivotal direction for the future optimization of site selection models.

6. Conclusion

Addressing the practical challenge of highly complex light environments in metropolitan fringe areas, this study used Guangzhou as a case study to integrate SDGSAT-1 nighttime light remote sensing, ground-based measurements, and POI-based social sensing data, and developed a framework for dark sky park site selection and light environment optimization applicable to highly urbanized regions. The main conclusions are as follows:

First, the study confirmed the existence of high-quality "dark sky islands" within the fringe areas of megacities. The comprehensive evaluation model identified a total of 13 nature protected areas with construction potential in the northeastern sector of Guangzhou. Notably, Conghua Lianxi Municipal Forest Park ranked first with a comprehensive suitability score of 0.89; field verification revealed a dominant zenith brightness of 20.4 mag/arcsec^2, with a maximum of 21.28 mag/arcsec^2 recorded during moonless early mornings, indicating that the night sky quality meets the Silver Tier standards of the Dark-Sky International and possesses exceptionally high value for conservation and utilization.

Second, the research revealed a unique mixed spatial pattern of "point-line-surface" light pollution in the urban fringe. The study discovered that, in addition to the conventional planar skyglow from towns (Liangkou Town), the luminous environment of the protected areas is subject to the superimposed effects of significant linear interference (the Shanzhan Expressway, located 2.5 km from the core area) and high-intensity internal point sources (public service facilities). Furthermore, night sky quality exhibits significant temporal dynamic characteristics, with the period from 02:00 to 05:00 identified as the optimal observational window.

Third, the study validated the effectiveness of the multi-source data fusion methodology in the analysis of complex luminous environments. In contrast to traditional single-source remote sensing monitoring, the approach proposed herein "macroscale remote sensing screening, microscale in-situ verification, and precise POI-based source tracing" significantly enhances the precision in analyzing spatially heterogeneous light pollution sources. This methodological system not only fills a gap in dark sky conservation research within highly urbanized regions but also provides a replicable quantitative paradigm for the Guangdong-Hong Kong-Macao Greater Bay Area and similar global megacities to excavate scarce dark sky resources during ecological civilization construction.

CRediT authorship contribution statement

Benyan Jiang: Writing – original draft, Conceptualization. **Kailing Xu:** Visualization, Data curation. **Zihao Zheng:** Writing – review & editing, Project administration. **Jianjun Li:** Project administration. **Hongguang Wang:** Writing – review & editing. **Lin Mei:** Methodology.

Declaration of competing interest

The authors declare that they have no known competing financial interests or personal relationships that could have appeared to influence the work reported in this paper.

Acknowledgements

This work was supported by the Guangdong Office of Philosophy and Social Science (No. GD24CGL48); the Basic and Applied Basic Research Foundation of Guangdong Province (No. 2023A1515110905); the Science and Technology Planning Project of Guangdong Province (No. 2024B1212080003) and the National Natural Science Foundation of China (No. 42401432; 42571537).

Data availability

Data will be made available on request.

References

Baack, F., Kuks, S.M., Özerol, G., Vinke-de Kruijf, J., Halman, J.I., 2024. Deciding climate change adaptation implementation at the local Level–a tale of two cities in the Netherlands. J. Environ. Plann. Manag. 1–21.
Bará, S., Bao-Varela, C., 2023. Skyglow inside your eyes: intraocular scattering and artificial brightness of the night sky. International Journal of Sustainable Lighting 25 (1), 1–9.
Bará, S., Falchi, F., Lima, R.C., Pawley, M., 2021. Keeping light pollution at bay: a red-lines, target values, top-down approach. Environ. Chall. 5, 100212.
Barentine, J.C., 2022. Night sky brightness measurement, quality assessment and monitoring. Nat. Astron. 6 (10), 1120–1132.
Chang, T.C., Tang, J.H., Chan, T.C., 2025. Spatiotemporal impact of urban development on nighttime light intensity and its hotspot distribution. PLoS One 20 (6), e0325696.
Chen, J., Xu, J., Zha, F., Wang, M., 2023. Suitability evaluation of site selection for the construction of dark sky parks in natural protected areas in Guangdong province. Chinese Landscape Architecture 39 (12), 120–126.
Dalgleish, H., 2021. Can we turn off the lights? Astron. Geophys. 62 (5), 5–16.

Das, K., Kumar, N., Devi, R.S., Rout, S., Majhi, S., Sharma, B.P., Kumar, S., 2025. Lost in the glow: how light pollution disrupts pollinator behavior. Asian Journal of Environment & Ecology 24 (12), 23–32.
Falchi, F., Bará, S., 2020. A linear systems approach to protect the night sky: implications for current and future regulations. R. Soc. Open Sci. 7 (12).
Falchi, F., Cinzano, P., Duriscoe, D., Kyba, C.C., Elvidge, C.D., Baugh, K., et al., 2016. The new world atlas of artificial night sky brightness. Sci. Adv. 2 (6), e1600377.
Feng, K., Dai, S., Hao, L., 2022. Preliminary study on the evolution characteristics of urban lighting pollution based on VllRS images: taking 4 Chinese cities as research objects. China Illuminating Engineering Journal 33 (4), 172–185.
Gagliardi, G., Lupia, M., Cario, G., Tedesco, F., Cicchello Gaccio, F., Lo Scudo, F., Casavola, A., 2020. Advanced adaptive street lighting systems for smart cities. Smart Cities 3 (4), 1495–1512.
Gaston, K.J., Sánchez, De. Miguel.A., 2022. Environmental impacts of artificial light at night. Annu. Rev. Environ. Resour. 47, 373–398.
Hirt, M.R., Evans, D.M., Miller, C.R., Ryser, R., 2023. Light pollution in complex ecological systems. Phil. Trans. Biol. Sci. 378 (1892).
Horynek, H., 2024. Convergence between increased light pollution and urban sprawl dynamic in Poland (2012–2022). Geomatics and Environmental Engineering 18 (6), 73–93.
Hung, L.W., Anderson, S.J., Pipkin, A., Fristrup, K., 2021. Changes in night sky brightness after a countywide LED retrofit. J. Environ. Manag. 292, 112776.
International Dark-Sky Association, 2018. International dark sky park program guidelines. https://www.darksky.org.
Jechow, A., Kolláth, Z., Ribas, S.J., Spoelstra, H., Hölker, F., Kyba, C.C., 2017. Imaging and mapping the impact of clouds on skyglow with all-sky photometry. Sci. Rep. 7 (1), 6741.
Jechow, A., Kyba, C.C., Hölker, F., 2019. Beyond all-sky: assessing ecological light pollution using multi-spectral full-sphere fisheye lens imaging. Journal of Imaging 5 (4), 46.
Jiang, W., He, G., Leng, W., Long, T., Wang, G., Liu, H., et al., 2018. Characterizing light pollution trends across protected areas in China using nighttime light remote sensing data. ISPRS Int. J. GeoInf. 7 (7), 243.
Jiang, B., Li, S., Li, J., Zhang, Y., Zheng, Z., 2022. Spatio-temporal dynamics and sensitive distance identification of light pollution in protected areas based on muti-source data: a case study of Guangdong province, China. Int. J. Environ. Res. Publ. Health 19 (19), 12662.
Jiang, B., Jian, S., Zheng, J., Li, J., Chen, J., 2026. Light disturbance of light shows on ecological spaces and its impact distance: a case study of the Guangzhou international light festival. Chin. J. Appl. Ecol. 1–12. https://doi.org/10.13287/j.1001-9332.202605.024.
Joye, W.A., Mandel, E., 2003. New features of SAOImage DS9. Astronomical Data Analysis Software and Systems XII 295, 489.
Kocifaj, M., Petržala, J., Medveď, I., 2024. Skyglow from ground-reflected radiation: model improvements. Mon. Not. Roy. Astron. Soc. 533 (2), 2356–2363.
Kyba, C.C., Kuester, T., Sánchez de Miguel, A., Baugh, K., Jechow, A., Hölker, F., et al., 2017. Artificially lit surface of Earth at night increasing in radiance and extent. Sci. Adv. 3 (11), e1701528.
Labrousse, C., Haspel, C., Levin, N., 2025. Quantifying the impact of the transition to LED lighting on night sky brightness and colour using ground-based measurements and satellite imagery. J. Quant. Spectrosc. Radiat. Transf. 340, 109450.
Li, X., Yeerleke, B., Zheng, J., Mei, L., 2025. Evaluation of the effectiveness of light pollution control in Shenzhen Xichong dark sky preserve based on nighttime light remote sensing. Trop. Geogr. 45 (8), 1373–1388.
Li, Z., Xing, R., Ling, Q., Wei, Z., Wang, Z., Ji, Q., Shi, K., 2026. Exploring global dark sky quality and potential dark sky park site selection: integrating multi-source spatial data with random forest model. Rem. Sens. Environ. 333, 115114.
Linares Arroyo, H., Abascal, A., Degen, T., Aubé, M., Espey, B.R., Gyuk, G., et al., 2024. Monitoring, trends and impacts of light pollution. Nat. Rev. Earth Environ. 5 (6), 417–430.
Liu, Z., Zhong, Y., Chen, Z., 2023. A study on the location of forest night park in Guangdong-Hong Kong-Macao Greater Bay Area based on multi-source data. Natural Protected Areas 3 (4), 89–102.
Liu, S., Wang, C., Chen, Z., Li, W., Zhang, L., Wu, B., et al., 2024. Efficacy of the SDGSAT-1 glimmer imagery in measuring sustainable development goal indicators 7.1. 1, 11.5. 2, and target 7.3. Rem. Sens. Environ. 305, 114079.
Liu, S., So, C.W., Pun, C.S.J., 2025. Analyzing the sources and variations of nighttime lights in Hong Kong from VIIRS monthly data. Remote Sens. 17 (8), 1447.
Navara, K.J., Nelson, R.J., 2007. The dark side of light at night: physiological, epidemiological, and ecological consequences. J. Pineal Res. 43 (3), 215–224.
Newbold, T., Hudson, L.N., Hill, S.L., Contu, S., Lysenko, I., Senior, R.A., et al., 2015. Global effects of land use on local terrestrial biodiversity. Nature 520 (7545), 45–50.
Robert, K.A., Dimovski, A.M., Contos, P., Khwaja, N., Griffiths, S.R., 2025. Divergent responses of insectivorous bats and flying insects to experimental LED illumination of different spectra. Ecosphere 16 (5), e70291.
Schneider, D., Schwalbe, E., Maas, H.G., 2009. Validation of geometric models for fisheye lenses. ISPRS J. Photogrammetry Remote Sens. 64 (3), 259–266.
Ściężor, T., Iwanicki, G., Kunz, M., Kotarba, A.Z., Skorb, K., Tabaka, P., 2025. Ecological light pollution (ELP) scale as a measure of light pollution impact on protected areas: case study of Poland. Sustainability 17 (11), 4824.
Shavkatov, S., 2023. Adaptive illumination: designing a smart street lighting system for sustainable urban environments. MATRIX Academic International Online Journal of Engineering and Technology 6 (1), 18–32.
So, C.W., Pun, C.S.J., Liu, S., 2025. Spectroscopic study of the light-polluted night sky in Hong Kong. J. Quant. Spectrosc. Radiat. Transf., 109696
Supriya, N., Kumar, S., 2023. Urban light plan-light pollution in urban areas & light pollution control. Int. J. Sci. Res. 12 (7), 651–655.
Tang, Q., Wang, C., Wang, Y., Su, R., Jiang, J., Cui, H., 2020. Preliminary study on light pollution monitoring based on volunteered passenger aircraft remote sensing. Remote Sensing Technology and Application 35 (6), 1360–1367.
Vardi-Naim, H., Benjamin, A., Sagiv, T., Kronfeld-Schor, N., 2022. Fitness consequences of chronic exposure to different light pollution wavelengths in nocturnal and diurnal rodents. Sci. Rep. 12 (1), 16486.
Wei, Y., Chen, Z., Xiu, C., Yu, B., Liu, H., 2019. Siting of dark sky reserves in China based on multi-source spatial data and multiple criteria evaluation method. Chin. Geogr. Sci. 29 (6), 949–961.
Wu, Y., Huang, C., Ye, Y., Mei, L., Liu, Y., Wang, D., et al., 2025. Identification and evaluation of nighttime light pollution in residential gathering area of megacities based on SDGSAT-1 glimmer imagery. Rem. Sens. Environ. 328, 114894.
Yang, L., Chen, J., Zhang, L., Zheng, Y., Yu, Y., Fu, Y., 2021. Study on the sleep effect of night light pollution based on remote sensing: a case study in Guangzhou City. Tropical Geomorphology 42 (1), 47–53.
Zheng, S., Chen, Y., Eziz, A., Kurban, A., Van de Voorde, T., De Maeyer, P., 2025. Machine-learning-based monitoring of night sky brightness using sky quality meters and multi-source remote sensing. Remote Sens. 17 (8), 1332.
Zhong, L., Yang, R., Zhao, Z., 2019. Half the park is after dark: america's experience and China's Route in the study of night skies. Landscape Architecture 26 (6), 85–90.
Zhu, A., Zhou, T., Zhong, Y., 2021. Development of dark night park in China: thinking on the study of dark night in global natural protected areas. Natural Protected Areas 1 (1), 42–51.